Microplankton Distribution in the California Current System - Preliminary Results

Barry and Evelyn Sherr, College of Oceanic & Atmospheric Sciences, Oregon State University, sherrb@coas.oregonstate.edu

Abstract: The goal of our project is to determine the distribution of microzooplankton (mainly ciliates and heterotrophic dinoflagellates) in the California Current System (CCS) as part of the 2001 – 2003 Long Term Observation Program (LTOP) off the Oregon and Northern Californian coasts. We are also assessing, via flow cytometry, the abundance distributions of heterotrophic bacteria, coccoid cyanobacteria, and eukaryotic algae in the CCS. During 3 spring-summer cruises (March, July, September) in 2001, we documented planktonic succession in coastal upwelling blooms. The first stage in newly upwelled water near the coast was dominated by large diatom blooms. Farther offshore, at the edge of the upwelling front, decaying diatom blooms were accompanied by intense blooms of coccoid cyanobacteria and nano- to pico-sized eukaryotic phytoplankton. Heterotrophic bacteria were also most abundant in this 'bloom decay' region. Both ciliates and heterotrophic dinoflagellates were found to be important components of the microzooplankton in the CCS. Ciliate biomass tended to be highest in the region of pico- and nano-phytoplankton blooms, while heterotrophic dinoflagellate biomass was also high in the inshore region of diatom blooms. Our preliminary conclusion is that the role of micro-zooplankton as grazers of phytoplankton and as food for mesozooplankton should be most important in the 'bloom decay' region of summer upwelling in the CCS.

Methods: Water samples were collected from six depths in the upper 100 m of the water column at stations along 5 transects (Figure 1) during LTOP cruises in 2001. In this report, we focus on the Newport Hydroline. Ciliates: samples were preserved with acid Lugol solution for settling and enumeration/sizing via inverted light microscopy. Heterotrophic dinoflagellates and other protists: samples were preserved with formalin, stained with DAPI, and settled onto 3.0 ¼m black-stained filters for enumeration via epifluorescence microscopy. Bacteria and phytoplankton: 3 ml samples were preserved with paraformaldehyde, quick-frozen and stored in liquid nitrogen until thawed and analysed using a Becton-Dickinson FACSCalibur flow cytometer. Coccoid cyanobacteria and eukaryotic phytoplankton were enumerated based on orange and red fluorescence of particles in unstained subsamples (Figure 2). Subsamples for bacterial counts were pre-treated with the nucleic acid stain SYBR-Green prior to flow cytometric analysis, and bacterial cells were enumerated based on green fluorescence and side-scatter properties (Figure 3). Distribution of microplankton was compared to sigma-t and in situ fluorescence profiles from LTOP CTD data collected on each cruise.

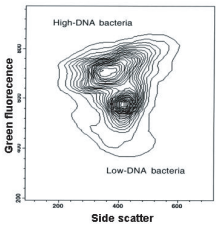

Figure 3. Contour plot of flow cytometric counts of heterotrophic bacteria in the CCS. Two groups of bacteria are commonly seen in such plots based on cell-specific DNA content

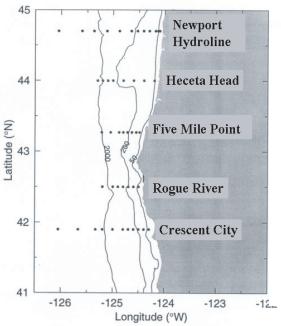

Figure 1. LTOP sampling transects in the CCS. The Newport Hydroline is sampled 5 times a year, the other transects only during the summer.

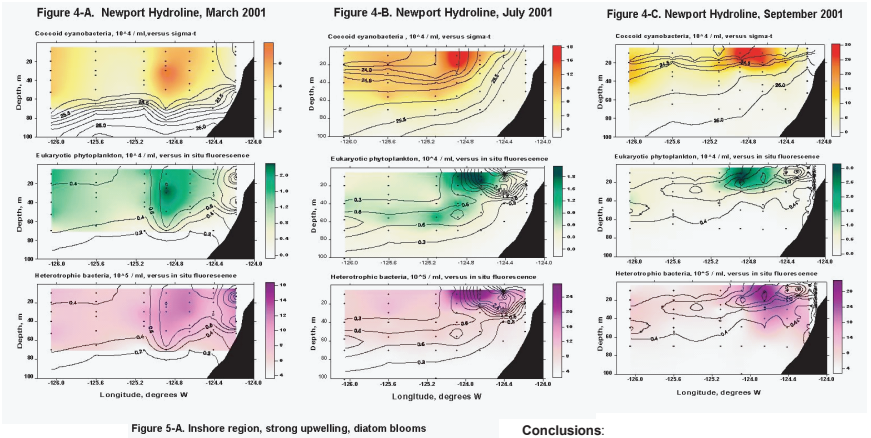

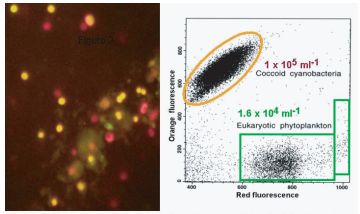

Figure 2. Cytogram of phytoplankton in water sample taken in July, Newport Hydroline, mid-shelf, 20 m depth. Micrograph shows yellow-orange-fluorescing cyanobacteria and red-fluorescing eukaryotic algae. For algae, fluorescence per cell is related to cell size.

Table 1. Abundance (cells/ml), average cell size (equivalent spherical diameter, ESD, µm), and biomass (ug C/liter) of ciliates and heterotrophic dinoflagellates along the Newport Line, January and March 2001. Values are mean ± one standard deviation. The proportion of dinoflagellate biomass to total ciliate + heterotrophic dinoflagellate biomass is also indicated.

Month	Ciliates			Heterotrophic Dinoflagellates			
	Cells/ml	ESD	µg C/liter	Cells/ml	ESD	µg C/liter	% of total
JAN	1.3 ± 0.5	37 ± 3	0.8 ± 0.5	10 ± 5	16 ± 13	0.8 ± 0.4	48 ± 17
MARCH	1.6 ± 0.5	36 ± 5	1.3 ± 0.8	10 ± 6	11 ± 12	0.3 ± 0.3	17 ± 13

Figure 6. A) 75 µm long ciliate stained with Lugol and visualized via inverted light microscopy, B) 66 µm long gyrodinoid dinoflagellate stained with DAPI and visualized via epifluorescence microscopy.

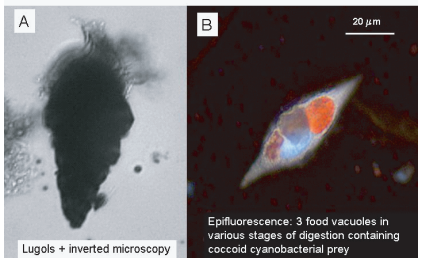

Figure 5-A. Inshore region, strong upwelling, diatom blooms

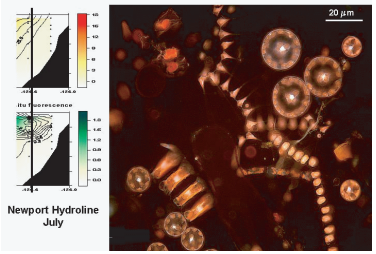

Figure 5-B. Midshelf region, decaying diatoms, blooms of pico- and nano-phytoplankton [center - copepod nauplius with ingested phytoplankton]

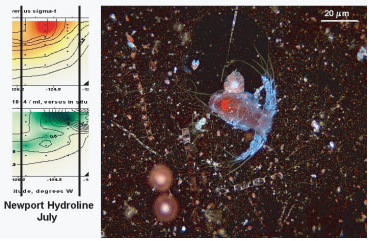

Figure 5-C. Outer shelf and slope, pico- and nano-plankton, low plankton abundances

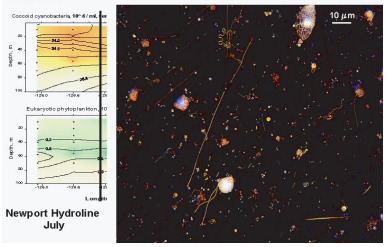

Conclusions:

1) **Two-stage upwelling blooms:** During the spring and summer, there was a consistent successional sequence to upwelling-induced blooms off the Oregon coast. Inshore blooms in newly upwelled water consisted mainly of a diverse assemblage of large centric diatoms. As the diatom blooms aged and decayed, intense blooms of nano- and pico- phytoplankton developed in the midshelf region, centered around the upwelling front. These blooms were accompanied by high abundances of heterotrophic bacteria.

2) **Ciliates and heterotrophic dinoflagellates are important components of the microzooplankton:** Ciliate abundances increased from March to July, and ciliates appeared to be mainly consuming pico- and nano-plankton sized prey. In July, ciliate abundances were highest in the midshelf region where blooms of small phytoplankton were most intense. Heterotrophic dinoflagellate abundance was highest in the region of diatom blooms in March; some dinoflagellates have extracellular feeding strategies that allow them to consume large-sized diatoms. Gyrodinoid dinoflagellates in the mid-shelf and offshore regions also appeared to be feeding on coccoid cyanobacteria and small algal cells.

3) **Three trophic regimes:** Our data suggest that in the CCS there are at least three trophic regimes:

A) **Inshore upwelling regime,** characterized by blooms of large-sized diatoms, where the microbial loop and nutrient recycling are relatively unimportant.

B) **Midshelf microbial loop regime,** where blooms of coccoid cyanobacteria, small eukaryotic phytoplankton, and bacteria occur, and where rates of protist grazing of both autotrophic and heterotrophic microbes, and of nutrient recycling, are high.

C) **Offshore oligotrophic regime,** where plankton abundances are low.

Sampling and analysis of data collected by us and others in the LTOP program over the next two years will allow us to confirm this initial assessment, and also to determine how mesozooplankton biomass is related microzooplankton biomass in these three regimes.

Acknowlegments: We thank Carlos Lopez for technical assistance in collection of the samples on cruises and for protist enumeration via inverted and epifluorescence microscopy; Brigette Stoffey, Linda Jauron-Mills, and Cidney Howard for assistance with ciliate enumeration via inverted microscopy; Lindsay Routt and Sarah Hay for data entry; and the crew of the R/V Wecoma and LTOP project personnel for invaluable support. This project is funded by NSF grant OCE-0101294 to B. & E. Sherr.

Results:

1) During all three cruises, we observed a mid-shelf region of intense blooms of coccoid cyanobacteria (1-3 x 10^5 cells/ml) and of eukaryotic phytoplankton (1-3 x 10^4 cells/ml) (Figure 4). These blooms were in the general region of the offshore upwelling front, based on sigma-t surfaces, and not in the region of highest in situ fluorescence. Bacterial abundances were highest in the mid-shelf bloom region. Seaward of the bloom region, over the outer shelf and slope, plankton abundances were low. Although we have focused on the Newport Hydroline here, similar phytoplankton abundance distributions were found for other LTOP transects in March and September.

2) Microscopic inspection of plankton in the inshore upwelling, pico- and nano-plankton blooms, and slope regions showed that large diatoms dominated the high-fluorescence zone in newly upwelled water (Figure 5-A), the mid-shelf plankton was characterized by decaying diatoms and high abundances of very small autotrophs and heterotrophic bacteria (Figure 5-B), and the slope region had low plankton abundances (Figure 5-C). The phytoplankton in the mid-shelf and slope regions included abundant pico-eukaryotic cells. Prasinophyte algae < 1 ¼m in size have been described off the California coast, and similar species are likely to occur in these waters.

3) Both ciliates and heterotrophic dinoflagellates were found to be important components of the microzooplankton community in the upper water column of the CCS (Figure 6-A&B). We have completed two data sets for microzooplankton abundance and biomass along the Newport Hydroline, in January and in March 2001 (Table 1). In January, microzooplankton biomass was equally divided between ciliates and heterotrophic dinoflagellates, but in March, the smaller average cell size of dinoflagellates lowered their average contribution to microzooplankton biomass to ~ 17%. In March, both ciliates and heterotrophic dinoflagellates were abundant in the inner shelf, diatom bloom region (Figure 7). In July, ciliate abundances ranged up to 9 cells/ml, and were highest in the midshelf region (Figure 8). Protists were frequently observed with food vacuoles containing coccoid cyanobacteria (e.g. Figure 6) and eukaryotic algae in epifluorescence samples.

Figure 7. Distribution of eukaryotic phytoplankton abundances, and of biomass of ciliates and of heterotrophic dinoflagellates, Newport Hydroline, March 2001

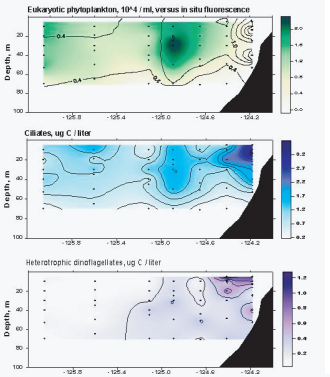

Figure 8. Abundance distribution of eukaryotic phytoplankton and of ciliates, Newport Hydroline, July 2001